ARS MATHEMATICA CONTEMPORANEA

ISSN 1855-3966 (printed edn.), ISSN 1855-3974 (electronic edn.)
ARS MATHEMATICA CONTEMPORANEA 16 (2019) 419–443
https://doi.org/10.26493/1855-3974.1401.7d9
(Also available at http://amc-journal.eu)

S^2 coverings by isosceles and scalene triangles – adjacency case I

Catarina P. Avelino *
Centre of Mathematics of the University of Minho – UTAD Pole (CMAT-UTAD), University of Trás-os-Montes e Alto Douro, Vila Real, Portugal
affiliated also with: *Center for Computational and Stochastic Mathematics (CEMAT), University of Lisboa (IST-UL), Portugal*

Altino F. Santos
Centre of Mathematics of the University of Minho – UTAD Pole (CMAT-UTAD), University of Trás-os-Montes e Alto Douro, Vila Real, Portugal

Received 9 May 2017, accepted 16 October 2017, published online 9 February 2019

Abstract

The aim of this paper is the study and classification of spherical f-tilings by scalene triangles T and isosceles triangles T'. Due to the complexity of this wide class of tilings, we consider a subclass performed by the adjacency of the shortest side of T and the longest side of T'. It consists of seven families of f-tilings (four families with one discrete parameter and one continuous parameter, two families with one discrete parameter and one sporadic f-tiling). We also analyze the combinatorial structure of all these families of f-tilings, as well as the group of symmetries of each tiling and the transitivity classes of isohedrality and isogonality.

Keywords: Dihedral f-tilings, combinatorial properties, spherical trigonometry, symmetry groups.
Math. Subj. Class.: 52C20, 52B05, 20B35

1 Introduction

A *folding tessellation* or *folding tiling* (f-tiling, for short) of the sphere S^2 is an edge-to-edge finite polygonal tiling τ of S^2 such that all vertices of τ satisfy the angle-folding relation, i.e., each vertex is of even valency and the sums of alternate angles around each vertex are equal to π.

*This research was partially supported by Fundação para a Ciência e a Tecnologia (FCT) through projects UID/MAT/00013/2013 and UID/Multi/04621/2013.

E-mail addresses: cavelino@utad.pt (Catarina P. Avelino), afolgado@utad.pt (Altino F. Santos)

F-tilings are intrinsically related to the theory of isometric foldings of Riemannian manifolds, introduced by Robertson [8] in 1977. In some situations (beyond the scope of this paper), the edge-complex associated to a spherical f-tiling is the set of singularities of some spherical isometric folding.

The classification of f-tilings was initiated by Breda [1], with a complete classification of all spherical monohedral (triangular) f-tilings. Afterwards, in 2002, Ueno and Agaoka [9] have established the complete classification of all triangular monohedral tilings of the sphere (without any restrictions on angles). Curiously, the triangular tilings of even valency at any vertex are necessarily f-tilings. Dawson has also been interested in special classes of spherical tilings, see [3, 4, 5], for instance. Spherical f-filings by two noncongruent classes of isosceles triangles have recently obtained [2, 7].

From now on,

(i) T denotes a spherical scalene triangle with internal angles $\alpha > \beta > \gamma$ and side lengths $a > b > c$;

(ii) T' denotes a spherical isosceles triangle with internal angles $(\delta, \delta, \varepsilon)$, $\delta \neq \varepsilon$, and side lengths (d, d, e),

as illustrated in Figure 1.

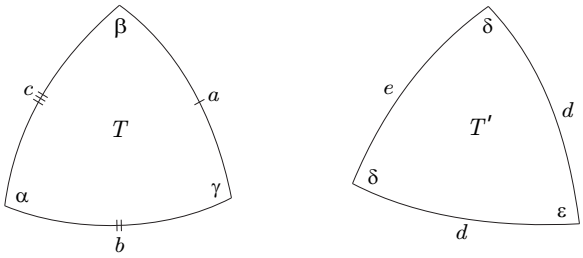

Figure 1: A spherical scalene triangle, T, and a spherical isosceles triangle, T'.

Taking into account the area of the prototiles T and T', we have

$$\alpha + \beta + \gamma > \pi \quad \text{and} \quad 2\delta + \varepsilon > \pi.$$

As $\alpha > \beta > \gamma$, we also have $\alpha > \frac{\pi}{3}$. In [6] it was established that any f-tiling by T and T' has necessarily vertices of valency four.

We begin by pointing out that any f-tiling by T and T', in which the shortest side of T is equal to the longest side of T', has at least two cells congruent to T and T', respectively, such that they are in adjacent positions and in one and only one of the situations illustrated in Figure 2. Our aim in this paper is to classify f-tilings in the first case of adjacency (Figure 2-Case I).

Next section contains the main results of this paper. In Subsection 2.1 we describe six families of spherical f-tilings and one single f-tiling that we may obtain in this case of adjacency. The combinatorial structure of these f-tilings and the classification of the group of symmetries and also the transitivity classes of isogonality and isohedrality are presented in Subsection 2.2. The proof of the main result consists in a long and exhaustive methodology and it is presented in Section 3.

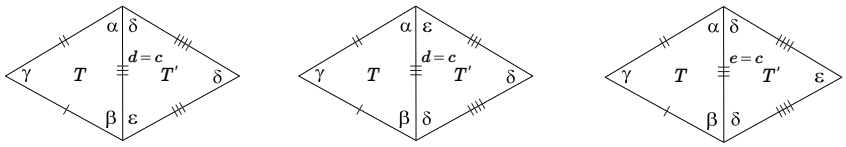

Case I: $\delta > \varepsilon$ Case II: $\delta < \varepsilon$

Figure 2: Distinct cases of adjacency.

2 Main result

2.1 f-tilings in the adjacency case I

Theorem 2.1. *Let T and T' be a spherical scalene triangle and a spherical isosceles triangle, respectively, such that they are in one of the adjacent positions illustrated in Figure 2-Case I. Then, from this we obtain six families of spherical f-tilings and one isolated f-tiling,*

$$\mathcal{D}^k_\delta\ (k\geq 3), \qquad \mathcal{G}^k\ (k\geq 4), \qquad \bar{\mathcal{G}}^k\ (k\geq 4), \qquad \mathcal{H},$$
$$\mathcal{F}^k_\beta\ (k\geq 4), \qquad \mathcal{I}^k_\beta\ (k\geq 3), \qquad \mathcal{J}^k_\beta\ (k\geq 4),$$

that satisfy, respectively:

(i) $\alpha+\delta=\pi,\ \delta+\beta+\varepsilon=\pi,\ k\gamma=\pi,\ \varepsilon=\varepsilon_k(\delta),\ \delta\in\left(\delta^k_{\min},\frac{\pi}{2}\right),\ k\geq 3$, *where*

$$\varepsilon_k(\delta)=2\,\mathrm{arccot}\left(2\cos\frac{\pi}{k}\csc 2\delta-\cot\delta\right) \quad \textit{and}$$
$$\delta^k_{\min}=\arccos\frac{\sqrt{1+8\cos\frac{\pi}{k}}-1}{4};$$

(ii) $\alpha+\delta=\pi,\ \alpha+\beta+\varepsilon=\pi,\ \delta+\beta+\gamma=\pi,\ k\gamma=\pi,\ \delta=\delta_k,\ k\geq 4$, *where*

$$\delta_k=\mathrm{arccot}\left(\frac{1}{2}\tan\frac{\pi}{2k}\left(2-\sec^2\frac{\pi}{2k}\right)\right);$$

(iii) $\alpha+\delta=\pi,\ \alpha+\beta+\varepsilon=\pi,\ \delta+\beta+\gamma=\pi,\ 2\beta+\gamma+\varepsilon=\pi,\ k\gamma=\pi,\ \delta=\delta_k,$ $k\geq 4$;

(iv) $\alpha+\delta=\pi,\ \alpha+\gamma+\gamma=\pi,\ 3\beta+\varepsilon=\pi,\ 5\gamma=\pi$, *where*

$$\beta=\beta^0=4\arctan\sqrt{3+4\sqrt{5}-2\sqrt{22+6\sqrt{5}}};$$

(v) $\alpha+\delta=\pi,\ 2\beta+\gamma+\varepsilon=\pi,\ k\gamma=\pi,\ \alpha=\alpha^1_k(\beta),\ \beta\in\left(\beta^{1k}_{\min},\beta^{1k}_{\max}\right),\ k\geq 4,$ *where*

$$\alpha^1_k(\beta)=\arccos\left(-\cos\frac{\pi}{k}\sec\frac{\pi}{2k}\cos\left(\beta+\frac{\pi}{2k}\right)\right),$$
$$\beta^{1k}_{\min}=\max\left\{\frac{\pi}{k},\arccos\left(\frac{1}{2}\sec\frac{\pi}{2k}\right)-\frac{\pi}{2k}\right\} \quad \textit{and}$$
$$\beta^{1k}_{\max}=\frac{(k-1)\pi}{2k};$$

(vi) $\alpha+\delta=\pi,\ 2\beta+\varepsilon=\pi,\ k\gamma=\pi,\ \alpha=\alpha_k^2(\beta),\ \beta\in\left(\beta_{\min}^{2k},\frac{\pi}{2}\right),\ k\geq 3$, *where*

$$\alpha_k^2(\beta)=\arccos\left(-\cos\frac{\pi}{k}\cos\beta\right)\quad \textit{and}$$
$$\beta_{\min}^{2k}=\max\left\{\frac{\pi}{k},\arccos\frac{\sqrt{\cos^2\frac{\pi}{k}+8}-\cos\frac{\pi}{k}}{4}\right\};$$

(vii) $\alpha+\varepsilon=\pi,\ \beta+2\delta=\pi,\ k\gamma=\pi,\ \alpha=\alpha_k^3(\beta),\ \beta\in\left(\frac{\pi}{k},\beta_{\max}^{3k}\right),\ k\geq 4$, *where*

$$\alpha_k^3(\beta)=\arccos\left(2\sin^2\frac{\beta}{2}-\cos\frac{\pi}{k}\right)\quad \textit{and}$$
$$\beta_{\max}^{3k}=2\arcsin\frac{\sqrt{1+8\cos\frac{\pi}{k}}-1}{4}.$$

For each family of f-tilings we present the distinct classes of congruent vertices in Figure 3 (including the respective number of vertices in each tiling).

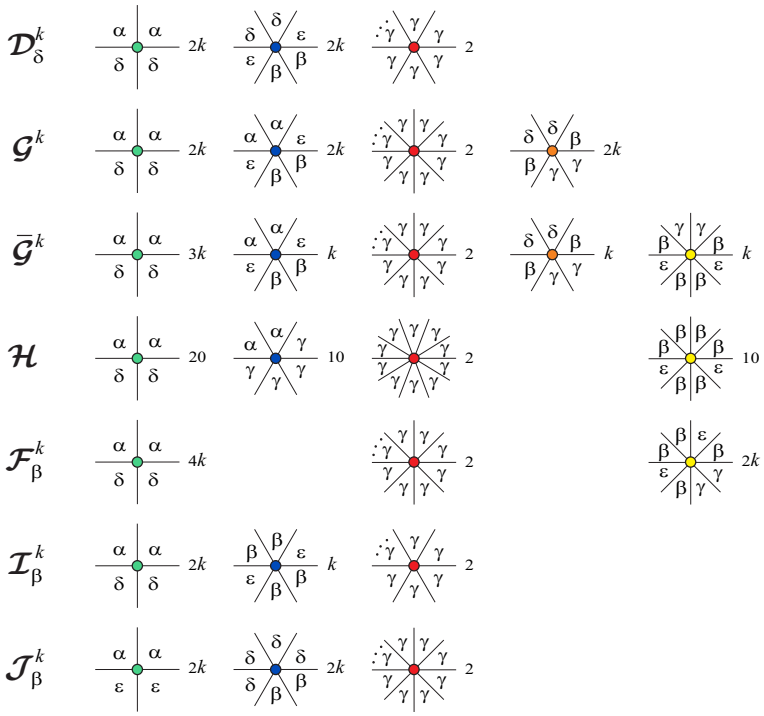

Figure 3: Distinct classes of congruent vertices.

Particularizing suitable values for the parameters involved in each case, the corresponding 3D representations of these families of f-tilings are given in Figures 4 – 10.

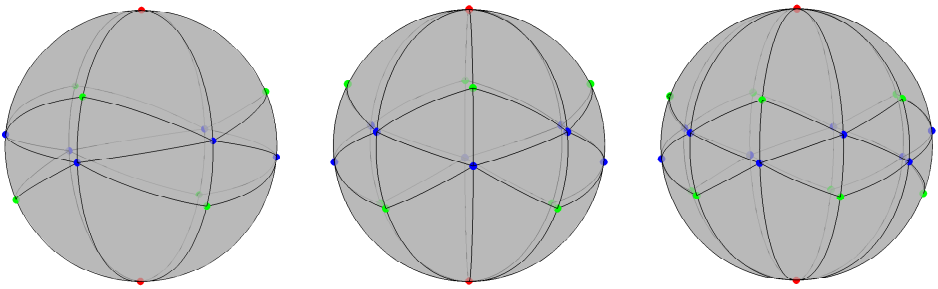

(a) $\mathcal{D}^3_\delta$ (b) $\mathcal{D}^4_\delta$ (c) $\mathcal{D}^5_\delta$

Figure 4: f-tilings in the adjacency case I; the $\mathcal{D}^k_\delta$ family.

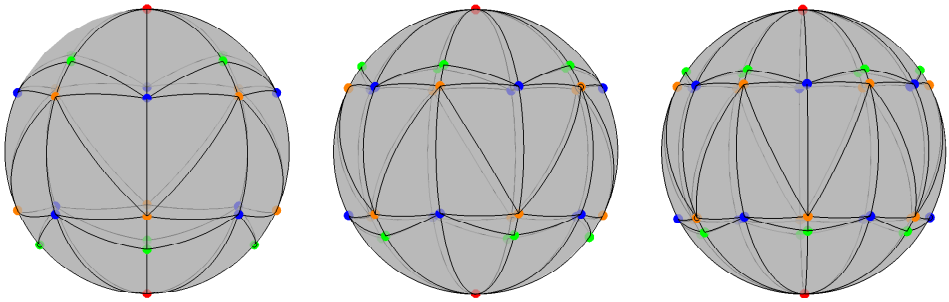

(d) $\mathcal{G}^4$ (e) $\mathcal{G}^5$ (f) $\mathcal{G}^6$

Figure 5: f-tilings in the adjacency case I; the $\mathcal{G}^k$ family.

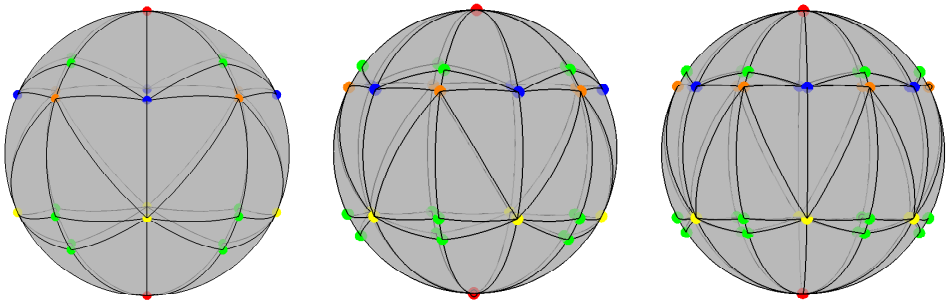

(g) $\bar{\mathcal{G}}^4$ (h) $\bar{\mathcal{G}}^5$ (i) $\bar{\mathcal{G}}^6$

Figure 6: f-tilings in the adjacency case I; the $\bar{\mathcal{G}}^k$ family.

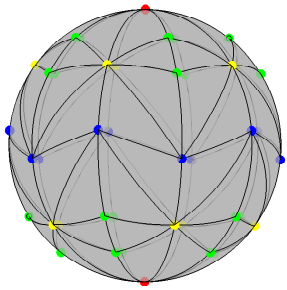

(j) $\mathcal{H}$

Figure 7: f-tilings in the adjacency case I; the isolated f-tiling.

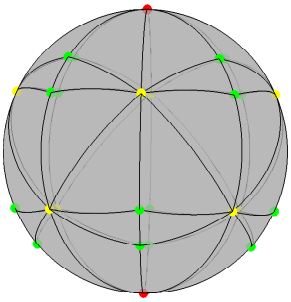

(k) $\mathcal{F}_\beta^4$

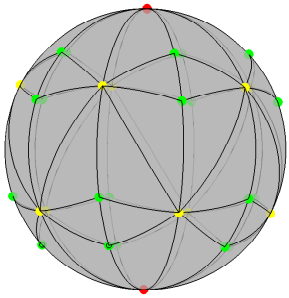

(l) $\mathcal{F}_\beta^5$

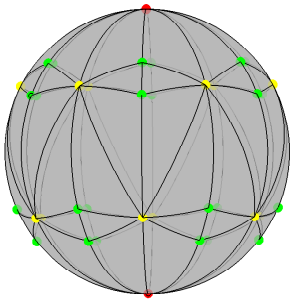

(m) $\mathcal{F}_\beta^6$

Figure 8: f-tilings in the adjacency case I; the $\mathcal{F}_\beta^k$ family.

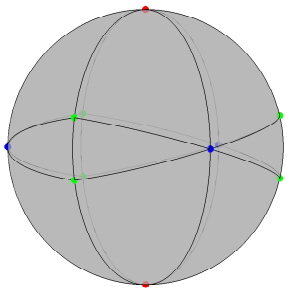

(n) $\mathcal{I}_\beta^3$

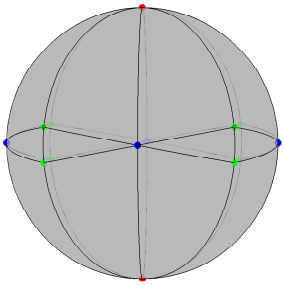

(o) $\mathcal{I}_\beta^4$

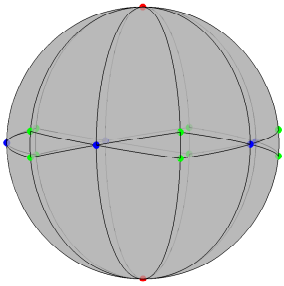

(p) $\mathcal{I}_\beta^5$

Figure 9: f-tilings in the adjacency case I; the $\mathcal{I}_\beta^k$ family.

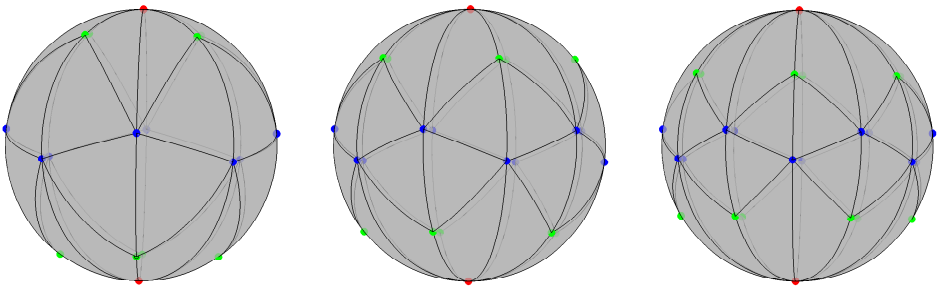

(q) $\mathcal{J}^4_\beta$ (r) $\mathcal{J}^5_\beta$ (s) $\mathcal{J}^6_\beta$

Figure 10: f-tilings in the adjacency case I; the $\mathcal{J}^k_\beta$ family.

2.2 Symmetry groups and combinatorial structure

In this subsection we present the group of symmetries of each spherical f-tiling mentioned in Theorem 2.1. The number of transitivity classes of tiles and vertices of each tiling is indicated in Table 1.

Any symmetry of $\mathcal{D}^k_\delta$, $k \geq 3$, fixes the north pole $N = (0, 0, 1)$ (and consequently the south pole $S = -N$) or maps N into S (and consequently S into N). The symmetries that fix N are generated, for instance, by the rotation $R^z_{\frac{2\pi}{k}}$ (of an angle $\frac{2\pi}{k}$ around the z axis) and the reflection ρ^{yz} (on the coordinate plane $y \circ z$) giving rise to a subgroup of $G(\mathcal{D}^k_\delta)$ isomorphic to D_k, the dihedral group of order $2k$. Now, the map

$$\phi = R^z_{\frac{\pi}{k}} \circ \rho^{xy} = \rho^{xy} \circ R^z_{\frac{\pi}{k}}$$

is a symmetry of $\mathcal{D}^k_\delta$ that changes N and S. One has $\phi^{2k-1} \circ \rho^{yz} = \rho^{yz} \circ \phi$ and ϕ has order $2k$. It follows that ϕ and ρ^{yz} generate $G(\mathcal{D}^k_\delta)$, and so it is isomorphic to D_{2k}. Moreover, $\mathcal{D}^k_\delta$ is 2-tile-transitive and 3-vertex-transitive with respect to this group.

The analysis considered to the combinatorial structure of $\mathcal{D}^k_\delta$ also applies to the family of f-tilings $\mathcal{G}^k$, $k \geq 4$. And so $G(\mathcal{G}^k) = D_{2k}$. $\mathcal{G}^k$ is 3-isohedral and 4-isogonal.

Concerning the family of f-tilings $\bar{\mathcal{G}}^k$, $k \geq 4$, we have that $G(\bar{\mathcal{G}}^k) = D_k$, since in this case there is no symmetry sending the north pole into the south pole. Moreover, $\bar{\mathcal{G}}^k$ has 6 transitivity classes of tiles, and so it is 6-isohedral. The vertices of $\bar{\mathcal{G}}^k$ form 8 transitivity classes.

Regarding the symmetry group of $\mathcal{H}$, the symmetries that fix N are generated by the rotation $R^z_{\frac{2\pi}{5}}$ and the reflection ρ^{yz} on the plane $x = 0$. On the other hand,

$$\phi = R^z_{\frac{\pi}{5}} \circ \rho^{xy}$$

is also a symmetry of $\mathcal{H}$ that sends N into S. Thus, we conclude that $G(\mathcal{H})$ is isomorphic to D_{10}, the dihedral group of order 20. $\mathcal{H}$ is 4-tile-transitive and 5-vertex-transitive.

Any symmetry of $\mathcal{I}^k_\beta$, $k \geq 3$, fixes N or maps N into S. The symmetries that fix N are generated, for instance, by the rotation $R^z_{\frac{2\pi}{k}}$ of order k and the reflection ρ^{yz}, giving rise to a subgroup $\mathcal{S}$ of $G(\mathcal{I}^k_\beta)$ isomorphic to D_k. To obtain the symmetries that send N into

S it is enough to compose each element of $\mathcal{S}$ with ρ^{xy}. Since ρ^{xy} commutes with $R^z_{\frac{\pi}{k}}$ and ρ^{yz}, we may conclude that $G(\mathcal{I}^k_\beta)$ is isomorphic to $C_2 \times D_k$. $\mathcal{I}^k_\beta$ has 2 transitivity classes of tiles with respect to the group of symmetries and 3 transitivity classes of vertices.

Similarly to previous cases, we have $G(\mathcal{F}^k_\beta) = G(\mathcal{J}^k_\beta) = D_{2k}$. $\mathcal{F}^k_\beta$ is 3-isohedral and 4-isogonal and $\mathcal{J}^k_\beta$ is 2-isohedral and 3-isogonal.

The combinatorial structure of the class of spherical f-tilings described in the previous subsection, including the symmetry groups, is summarized in Table 1. Our notation is as follows:

- $|V|$ is the number of distinct classes of congruent vertices;
- N_1 and N_2 are, respectively, the number of triangles congruent to T and T', respectively;
- $G(\tau)$ is the symmetry group of each tiling τ and the indices of isohedrality and isogonality for the symmetry group are denoted, respectively, by #isoh. and #isog.

3 Proof of Theorem 2.1

In the case of adjacency I, any f-tiling by T and T' has at least two cells congruent to T and T', respectively, such that they are in adjacent positions and in one and only one of the situations illustrated in Figure 2. After certain initial assumptions are made, it is usually possible to deduce sequentially the nature and orientation of most of the other tiles. Eventually, either a complete tiling or an impossible configuration proving that the hypothetical tiling fails to exist is reached. In the diagrams that follow, the order in which these deductions can be made is indicated by the numbering of the tiles. For $j \geq 2$, the location of tiling j can be deduced directly from the configurations of tiles $(1, 2, \ldots, j-1)$ and from the hypothesis that the configuration is part of a complete f-tiling, except where otherwise indicated.

Observe that we have $\delta > \frac{\pi}{3}$. Also, as $d = c$ and using spherical trigonometric formulas, we get

$$\frac{\cos\gamma + \cos\alpha\cos\beta}{\sin\alpha\sin\beta} = \cot\delta\cot\frac{\varepsilon}{2}. \tag{3.1}$$

Proof of Theorem 2.1. We consider separately the subcases illustrated in Figure 2-Case I.

Case I.1: With the labeling of Figure 11(a), at vertex v_1 we must have

$$\alpha + \delta < \pi \quad \text{or} \quad \alpha + \delta = \pi.$$

Case I.1.1: Suppose firstly that $\alpha + \delta < \pi$. If $\alpha < \delta$, we must have $\alpha + \delta + k\varepsilon = \pi$, with $k \geq 1$. Due to the existence of vertices of valency four, it follows that $\delta = \frac{\pi}{2}$, and consequently, by Equation (3.1), $\cos\gamma + \cos\alpha\cos\beta = 0$. Nevertheless, this is not possible, since $\cos\gamma > \cos\beta > \cos\alpha > 0$. Therefore, $\alpha \geq \delta$. It follows that $\alpha > \beta > \delta > \varepsilon > \gamma$ and $\alpha + \delta + k\gamma = \pi$, with $k \geq 1$; see Figure 11(b). Note that $\theta_1 = \gamma$, otherwise at vertex v_2 we get $\alpha + \beta = \pi = \gamma + \varepsilon$, which is an impossibility. Now, we have

$$\theta_2 = \gamma, \quad \theta_2 = \delta \quad \text{or} \quad \theta_2 = \varepsilon.$$

Case I.1.1.1: If $\theta_2 = \gamma$, we obtain the configuration illustrated in Figure 12(a). Due to the edge lengths, at vertex v_3 we must have $\theta_3 + \beta + \rho \leq \pi$, with $\rho \geq \varepsilon$, which implies $\theta_3 = \varepsilon$. At vertex v_4 we reach a contradiction, as $\alpha + \delta + \rho > \pi$, for all $\rho \in \{\alpha, \beta, \delta, \varepsilon\}$.

Table 1: Combinatorial structure of the dihedral f-tilings of S^2 by scalene triangles T and isosceles triangles T' performed by the shortest side of T and the longest side of T' in the case of adjacency I.

f-tiling	$\boldsymbol{\alpha}$	$\boldsymbol{\beta}$	$\boldsymbol{\gamma}$	$\boldsymbol{\delta}$	$\boldsymbol{\varepsilon}$	$\lvert V\rvert$	N_1	N_2	$G(\tau)$	**#isoh.**	**#isog.**
$\boldsymbol{\mathcal{D}^k_\delta,\ k\geq 3}$	$\pi-\delta$	$\pi-\delta-\varepsilon$	$\frac{\pi}{k}$	$\left(\delta^k_{\min},\frac{\pi}{2}\right)$	$\varepsilon_k(\delta)$	3	$4k$	$4k$	D_{2k}	2	3
$\boldsymbol{\mathcal{G}^k,\ k\geq 4}$	$\pi-\delta$	$\frac{(k-1)\pi}{k}-\delta$	$\frac{\pi}{k}$	δ_k	$2\delta-\frac{(k-1)\pi}{k}$	4	$8k$	$4k$	D_{2k}	3	4
$\boldsymbol{\bar{\mathcal{G}}^k,\ k\geq 4}$	$\pi-\delta$	$\frac{(k-1)\pi}{k}-\delta$	$\frac{\pi}{k}$	δ_k	$2\delta-\frac{(k-1)\pi}{k}$	5	$8k$	$4k$	D_k	6	8
$\boldsymbol{\mathcal{H}}$	$\frac{3\pi}{5}$	β^0	$\frac{\pi}{5}$	$\frac{2\pi}{5}$	$\pi-3\beta^0$	4	60	20	D_{10}	4	5
$\boldsymbol{\mathcal{F}^k_\beta,\ k\geq 4}$	$\alpha^1_k(\beta)$	$\left(\beta^{1k}_{\min},\beta^{1k}_{\max}\right)$	$\frac{\pi}{k}$	$\pi-\alpha$	$\frac{(k-1)\pi}{k}-2\beta$	3	$8k$	$4k$	D_{2k}	3	4
$\boldsymbol{\mathcal{I}^k_\beta,\ k\geq 3}$	$\alpha^2_k(\beta)$	$\left(\beta^{2k}_{\min},\frac{\pi}{2}\right)$	$\frac{\pi}{k}$	$\pi-\alpha$	$\pi-2\beta$	3	$4k$	$2k$	$C_2\times D_k$	2	3
$\boldsymbol{\mathcal{J}^k_\beta,\ k\geq 4}$	$\alpha^3_k(\beta)$	$\left(\frac{\pi}{k},\beta^{3k}_{\max}\right)$	$\frac{\pi}{k}$	$\frac{\pi-\beta}{2}$	$\pi-\alpha$	3	$4k$	$4k$	D_{2k}	2	3

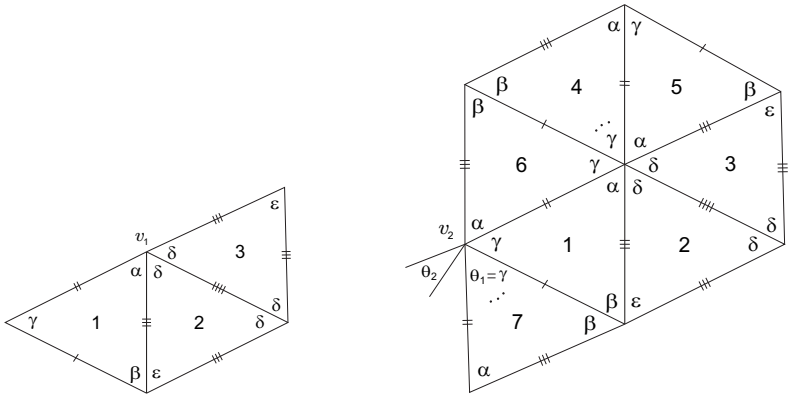

Figure 11: Local configurations.

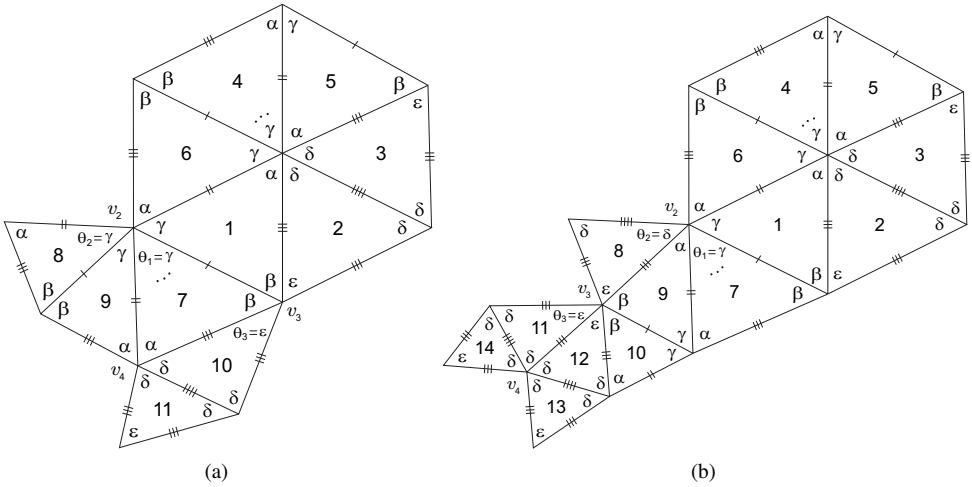

Figure 12: Local configurations.

Case I.1.1.2: If $\theta_2 = \delta$ (Figure 12(b)), we reach an impossibility at vertex v_4, since $\delta + \delta + \rho > \pi$, for all $\rho \in \{\alpha, \beta, \delta, \varepsilon\}$. Note that θ_3 cannot be γ (tile 11), as it implies a sum of alternate angles at vertex v_3 including the angles β, ρ_1 and ρ_2, with $\rho_1 \in \{\alpha, \beta\}$ and $\rho_2 \in \{\alpha, \beta, \delta, \varepsilon\}$, which is not possible due to the dimensions of the involved angles.

Case I.1.1.3: Finally we consider $\theta_2 = \varepsilon$ (Figure 13(a)). At vertex v_3 we must have $\delta + \beta + \bar{k}\gamma = \pi$, $\bar{k} > k$. Nevertheless, an incompatibility between sides at this vertex cannot be avoided.

Case I.1.2: Suppose now that $\alpha + \delta = \pi$ (consequently $\beta + \gamma > \delta > \frac{\pi}{3}$). If $\alpha = \delta = \frac{\pi}{2}$, we also get $\gamma = \frac{\pi}{2}$, which is not possible. On the other hand, if $\delta > \frac{\pi}{2} > \alpha\,(> \beta > \gamma)$, we obtain $\cot \delta < 0$, thereby making Equation (3.1) infeasible. Thus, $\alpha > \frac{\pi}{2} > \delta$. With the

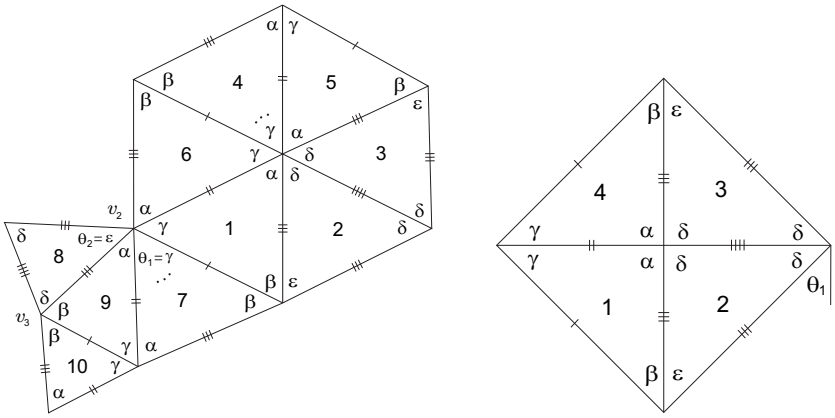

Figure 13: Local configurations.

labeling of Figure 13(b), we have

$$\theta_1 = \delta, \quad \theta_1 = \varepsilon, \quad \theta_1 = \beta \quad \text{or} \quad \theta_1 = \alpha.$$

Case I.1.2.1: If $\theta_1 = \delta$, we get the configuration illustrated in Figure 14(a). Note that, at vertex v_2, it is not possible to have $\delta + \delta + k\gamma = \pi$, with $k \geq 1$, and $\delta + \delta + \beta + \gamma > \pi$. At vertex v_3 we must have $\alpha + \beta + k\varepsilon = \pi$, with $k \geq 1$. Nevertheless, at this vertex we

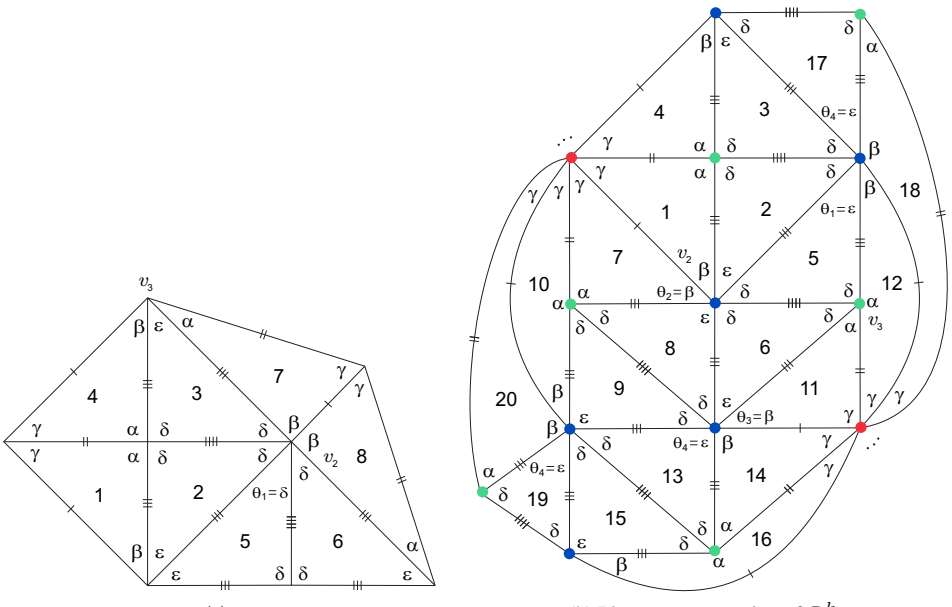

Figure 14: Local configurations.

reach a contradiction, since $(\delta+\delta+\beta)+(\alpha+\beta+\varepsilon) > (\delta+\delta+\varepsilon)+(\alpha+\beta+\gamma) > 2\pi$.

Case I.1.2.2: If $\theta_1 = \varepsilon$, we obtain the configuration of Figure 14(b). Note that if $\theta_2 = \gamma$, we would get the angles $(\delta, \varepsilon, \gamma, \beta, \dots)$ in one of the sum of alternate angles at vertex v_2; but $(\delta+\varepsilon+\gamma+\beta)+(\alpha+\delta) = (\delta+\delta+\varepsilon)+(\alpha+\beta+\gamma) > 2\pi$, which is not possible; at tile 11, it is easy to observe that $\theta_3 \neq \alpha, \gamma, \delta$; on the other hand, θ_3 cannot be ε, otherwise, at vertex v_3, we get $\delta+\delta+\beta = \pi$, but $(\alpha+\delta)+(\delta+\delta+\beta)+(\varepsilon+\delta+\beta+\varepsilon+\cdots) > 2(\delta+\delta+\varepsilon)+(\alpha+\beta+\gamma) > 3\pi$, which is a contradiction; a similar reasoning applies to the choice of θ_4 and the fact that $\bar{k} = 1$ in the sum $\delta+\beta+\bar{k}\varepsilon = \pi$, at vertex v_2. We denote the continuous family of f-tilings illustrated in Figure 14(b) by $\mathcal{D}_\delta^k$, where

$$\alpha+\delta = \pi, \quad \delta+\beta+\varepsilon = \pi \quad \text{and} \quad k\gamma = \pi, \text{ with } k \geq 3.$$

As $0 < \varepsilon < \delta < \frac{\pi}{2}$, using Equation (3.1) we get

$$\begin{aligned}
\frac{\cos\frac{\pi}{k}+\cos\delta\cos(\delta+\varepsilon)}{\sin(\delta+\varepsilon)} = \frac{\cos\delta\cos\frac{\varepsilon}{2}}{\sin\frac{\varepsilon}{2}} &\iff \cos\frac{\pi}{k}\sin\frac{\varepsilon}{2} = \cos\delta\sin\left(\delta+\frac{\varepsilon}{2}\right)\\
&\iff \cos\frac{\pi}{k} = \cos\delta\sin\delta\cot\frac{\varepsilon}{2}+\cos^2\delta\\
&\iff \cot\frac{\varepsilon}{2} = 2\cos\frac{\pi}{k}\csc 2\delta - \cot\delta.
\end{aligned}$$

Therefore,

$$\varepsilon = \varepsilon_k(\delta) = 2\,\mathrm{arccot}\left(2\cos\frac{\pi}{k}\csc 2\delta - \cot\delta\right),\ k \geq 3,$$

with $\delta \in \left(\delta_{\min}^k, \frac{\pi}{2}\right)$, where

$$\delta_{\min}^k = \arccos\frac{\sqrt{1+8\cos\frac{\pi}{k}}-1}{4} > \frac{\pi}{3}$$

is obtained when $\varepsilon = \delta$. The graph of this function for $\delta_{\min}^k < \delta < \frac{\pi}{2}$ is outlined in Figure 15, for different values of k. 3D representations of $\mathcal{D}_\delta^3$, $\mathcal{D}_\delta^4$ and $\mathcal{D}_\delta^5$ are given in Figures 4(a)–4(c).

Case I.1.2.3: Consider $\theta_1 = \beta$ (Figure 16(a)). At vertex v_1 we cannot have $\alpha+\beta = \pi = \varepsilon+\gamma$, as $\alpha > \delta > \varepsilon$ and $\beta > \gamma$. Thus, $\alpha > \frac{\pi}{2} > \delta > \beta > \gamma > \varepsilon$ and $\alpha+\beta+k\varepsilon = \pi$, $k \geq 1$. It is easy to observe that $k = 1$, as $k > 1$ lead to a vertex with a sum of alternate angles including the angles δ, δ and ρ, with $\rho \in \{\alpha, \beta, \delta, \varepsilon\}$, which is not possible due to the dimensions of the involved angles. The last configuration extends to the one illustrated in Figure 16(b). At vertex v_2 we have necessarily one of the following situations:

(i) $\delta+\beta+\beta = \pi$;

(ii) $\delta+\beta+\gamma = \pi$.

Note that $\delta+\beta+k\varepsilon = \pi$, $k > 1$ lead to a vertex with a sum of alternate angles including the angles δ, δ and ρ, with $\rho \in \{\alpha, \beta, \delta, \varepsilon\}$.

(i) If $\delta+\beta+\beta = \pi$, we obtain the configuration illustrated in Figure 17(a). Note that, at vertex v_3, we cannot have $\alpha+\gamma+\gamma+k\rho = \pi$, with $\rho \in \{\gamma, \varepsilon\}$ and $k \geq 1$, otherwise we get $(\alpha+\gamma+\gamma+k\rho)+(\alpha+\delta)+(\delta+\beta+\beta) \geq (\alpha+\beta+\gamma)+(\alpha+\beta+\gamma)+(\delta+\delta+\varepsilon) > 3\pi$, which is not possible.

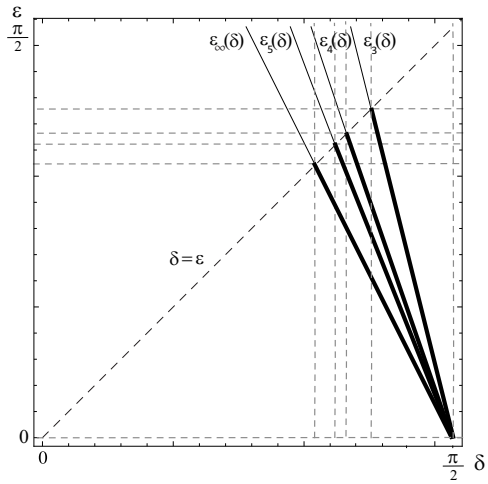

Figure 15: $\varepsilon = \varepsilon_k(\delta)$, with $\delta^k_{\min} < \delta < \frac{\pi}{2}$, and for $k = 3, 4, 5, \ldots, \infty$.

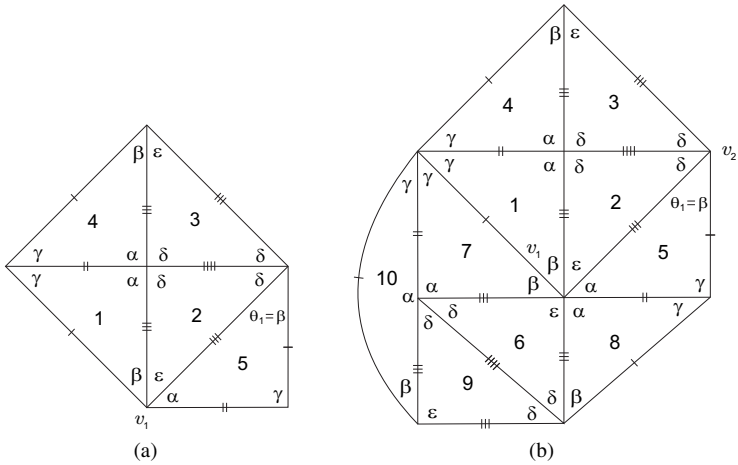

Figure 16: Local configurations.

At vertex v_4 we must have $k\gamma = \pi$, with $k \geq 4$. As $\delta = 2\gamma$ and $\pi < \delta + \delta + \varepsilon = 4\gamma + \varepsilon$, we conclude that $k = 4$, which is not possible as $\delta < \frac{\pi}{2}$.

(ii) If $\delta + \beta + \gamma = \pi$, the last configuration gives rise to the one illustrated in Figure 17(b), where θ_2 can be ε or δ. According to the selection for θ_2, we obtain the planar representations illustrated in Figures 18(a) and 18(b), respectively. In the first case we have

$$\alpha + \delta = \pi, \quad \alpha + \beta + \varepsilon = \pi, \quad \delta + \beta + \gamma = \pi, \quad k\gamma = \pi, \text{ with } k \geq 4,$$

and

$$\delta = \delta_k = \operatorname{arccot}\left(\frac{1}{2}\tan\frac{\pi}{2k}\left(2 - \sec^2\frac{\pi}{2k}\right)\right).$$

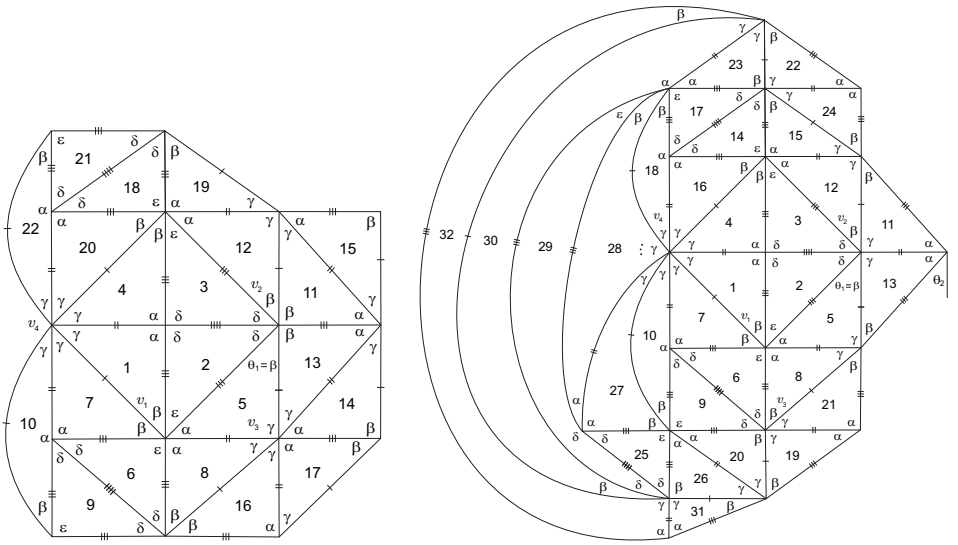

(a) (b)

Figure 17: Local configurations.

Note that by Equation (3.1) we have

$$\begin{aligned}\frac{\cos\frac{\pi}{k}+\cos\delta\cos(\delta+\frac{\pi}{k})}{\sin(\delta+\frac{\pi}{k})} &= -\frac{\cos\delta\sin\left(\delta+\frac{\pi}{2k}\right)}{\cos\left(\delta+\frac{\pi}{2k}\right)}\\ &\iff \cos\frac{\pi}{k}\cos\left(\delta+\frac{\pi}{2k}\right)+\cos\delta\cos\frac{\pi}{2k}=0\\ &\iff 2\cos\delta\cos^3\frac{\pi}{2k}-\sin\delta\cos\frac{\pi}{k}\sin\frac{\pi}{2k}=0\\ &\iff \cot\delta=\tan\frac{\pi}{2k}-\frac{1}{2}\tan\frac{\pi}{2k}\sec^2\frac{\pi}{2k}.\end{aligned}$$

We denote this family of f-tilings by $\mathcal{G}^k$, $k\geq 4$. 3D representations of $\mathcal{G}^k$, $k=4,5,6$, are presented in Figures 5(d) – 5(f).

In the second case we have

$$\begin{aligned}&\alpha+\delta=\pi,\quad \alpha+\beta+\varepsilon=\pi,\quad \delta+\beta+\gamma=\pi,\quad 2\beta+\gamma+\varepsilon=\pi,\\ &k\gamma=\pi,\ \text{with } k\geq 4,\quad \text{and } \delta=\delta^k;\end{aligned}$$

we denote this family of f-tilings by $\bar{\mathcal{G}}^k$. 3D representations, for $k=4,5,6$, are presented in Figures 6(g) – 6(i).

Case I.1.2.4: If $\theta_1=\alpha$ (Figure 19(a)), we must have $\beta<\delta$, otherwise there is no way to satisfy the angle-folding relation around vertex v_1. Then, $\alpha>\frac{\pi}{2}>\delta>\beta>\gamma$ and $\delta>\varepsilon$. Now, we have

$$\theta_2=\beta,\quad \theta_2=\gamma\quad\text{or}\quad \theta_2=\varepsilon.$$

Note that θ_2 cannot be δ, as $\delta+\beta+\varepsilon+\rho>\pi$, for all $\rho\in\{\beta,\gamma\}$.

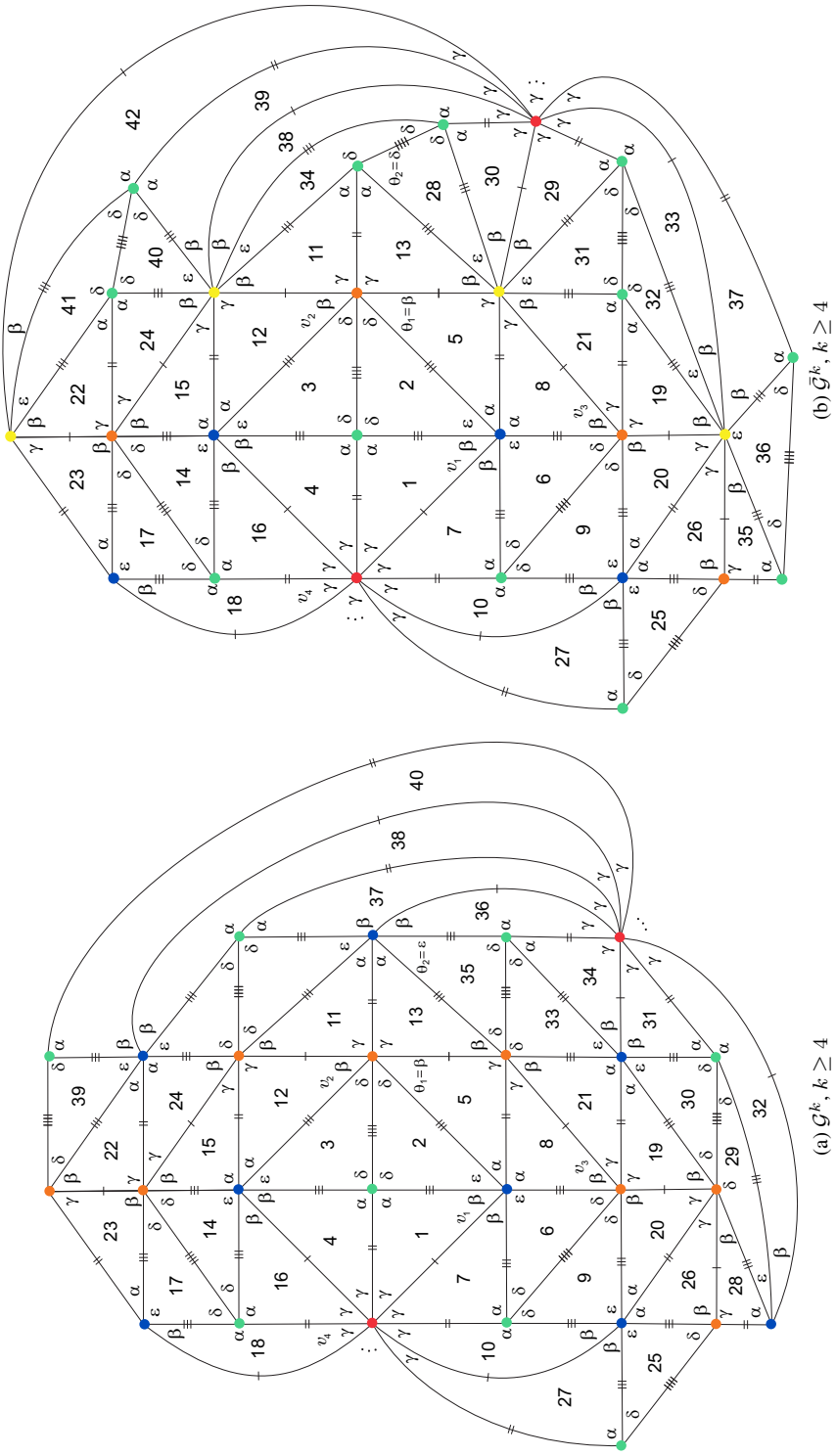

(a) $\mathcal{G}^k$, $k \geq 4$ (b) $\bar{\mathcal{G}}^k$, $k \geq 4$

Figure 18: Planar representations.

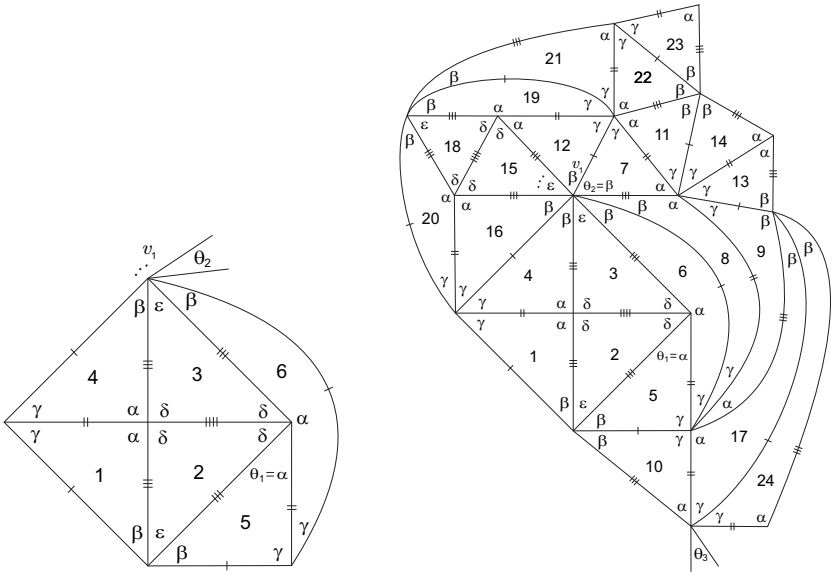

Figure 19: Local configurations.

Case I.1.2.4.1: If $\theta_2 = \beta$, we get the configuration illustrated in Figure 19(b), where $\alpha + 2\gamma = \pi$ and, at vertex v_1, $3\beta + k\varepsilon = \pi$, $k \geq 1$. As $k > 1$ implies the existence of a vertex with a sum of alternate angles containing $\delta + \delta + \beta$, and $(3\beta + k\varepsilon) + (2\delta + \beta) + (\alpha + \delta) \geq (\alpha + \beta + \gamma) + 2(2\delta + \varepsilon) > 3\pi$, we conclude that $k = 1$. Now, $\theta_3 \in \{\varepsilon, \gamma\}$. If $\theta_3 = \varepsilon$ (Figure 20(a)), at vertex v_2 we reach a contradiction, as for $\rho \in \{\beta, \gamma\}$, we get $\delta + \beta + \varepsilon + \rho \geq \delta + \beta + \varepsilon + \gamma > 2\delta + \varepsilon > \pi$. On the other hand, if $\theta_3 = \gamma$, the last configuration extends to the one illustrated in Figure 20(b).

If $\theta_4 = \varepsilon$ (Figure 21(a)), at vertex v_3 we must have $\delta + 2\beta = \pi$, as $\delta + 2\beta + \rho > \pi$, for all $\rho \in \{\alpha, \beta, \gamma, \delta, \varepsilon\}$ (note that $\alpha + \beta + \varepsilon = 3\beta + \varepsilon = \pi$, implying $\gamma > \varepsilon$; consequently $\alpha > \frac{\pi}{2} > \delta > \beta > \gamma > \varepsilon$). As $k\gamma = \pi$, $4\gamma = \delta + 2\gamma < \alpha + 2\gamma = \pi$ and $6\gamma = 3\delta > \pi$, we conclude that $k = 5$. Jointly with the remaining conditions, we obtain $\alpha = \frac{3\pi}{5}$, $\beta = \frac{3\pi}{10}$, $\gamma = \frac{\pi}{5}$, $\delta = \frac{2\pi}{5}$ and $\varepsilon = \frac{\pi}{10}$. Nevertheless, under these conditions, Equation (3.1) is impossible. On the other hand, if $\theta_4 = \delta$, we obtain the planar representation illustrated in Figure 21(b). We have

$$\alpha = \frac{3\pi}{5}, \quad \beta = 4\arctan\sqrt{3 + 4\sqrt{5} - 2\sqrt{22 + 6\sqrt{5}}},$$
$$\gamma = \frac{\pi}{5}, \quad \delta = \frac{2\pi}{5}, \quad \text{and} \quad \varepsilon = \pi - 3\beta.$$

We denote this f-tiling by $\mathcal{H}$, whose 3D representation is presented in Figure 7(j).

Case I.1.2.4.2: If $\theta_2 = \gamma$, we obtain the configuration illustrated in Figure 22(a). Note that, at vertex v_1, all the alternate angle sums containing $\beta+\beta+\gamma+\rho$, with $\rho \in \{\alpha, \beta, \gamma, \delta\}$, exceed π, and so $\beta + \beta + \gamma + k\varepsilon = \pi$, with $k = 1$ ($k \geq 1$ implies the existence of a vertex with alternate sum $\delta + \delta + \beta = \pi$ and $\varepsilon > \beta$).

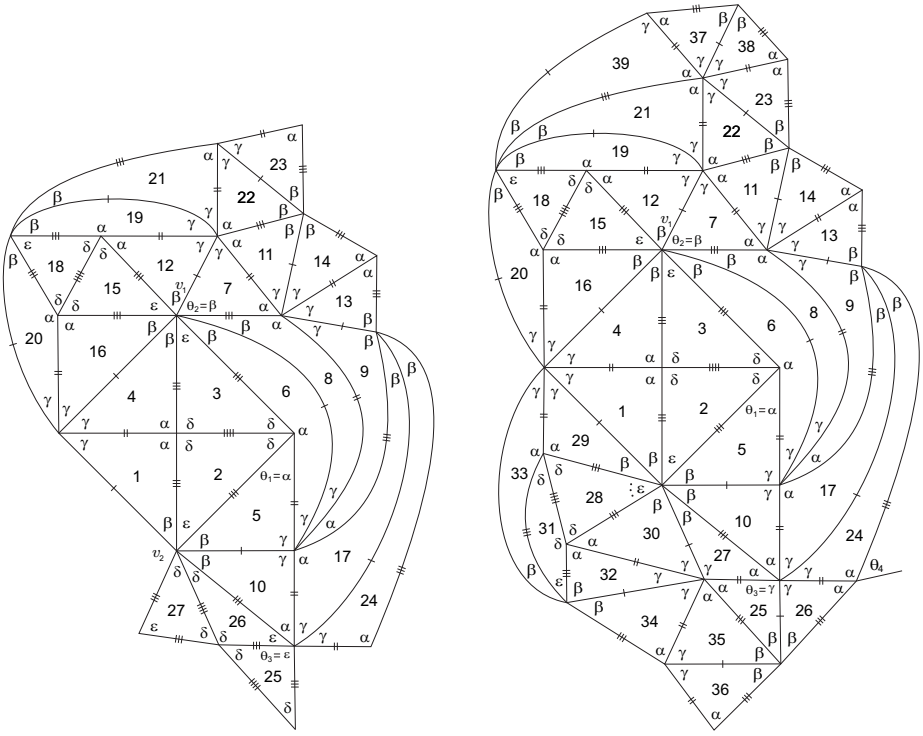

Figure 20: Local configurations.

Now, θ_3 must be β or γ.

In the first case (Figure 22(b)), we observe that at vertex v_3 we must have $\delta+\delta+\beta=\pi$, implying at vertex v_4 the existence of an alternate angle sum containing $\alpha+\beta+\gamma>\pi$, which is an impossibility.

On the other hand, if $\theta_3=\gamma$, the last configuration extends to the one illustrated in Figure 23. We denote this family of f-tilings by $\mathcal{F}^k_\beta$, where

$$\alpha+\delta=\pi, \quad 2\beta+\gamma+\varepsilon=\pi \quad \text{and} \quad k\gamma=\pi, \text{ with } k\geq 4.$$

As $\gamma=\frac{\pi}{k}<\beta<\delta$, $\beta+\gamma>\delta$, using Equation (3.1) we get

$$\begin{aligned}\frac{\cos\frac{\pi}{k}+\cos\alpha\cos\beta}{\sin\beta} &= \frac{-\cos\alpha\sin\left(\beta+\frac{\pi}{2k}\right)}{\cos\left(\beta+\frac{\pi}{2k}\right)}\\ &\iff \cos\frac{\pi}{k}\cos\left(\beta+\frac{\pi}{2k}\right)+\cos\alpha\cos\frac{\pi}{2k}=0\\ &\iff \cos\alpha=-\cos\frac{\pi}{k}+\sec\frac{\pi}{2k}\cos\left(\beta+\frac{\pi}{2k}\right).\end{aligned}$$

Therefore,

$$\alpha=\alpha_k^1(\beta)=\arccos\left(-\cos\frac{\pi}{k}\sec\frac{\pi}{2k}\cos\left(\beta+\frac{\pi}{2k}\right)\right),\ k\geq 4,$$

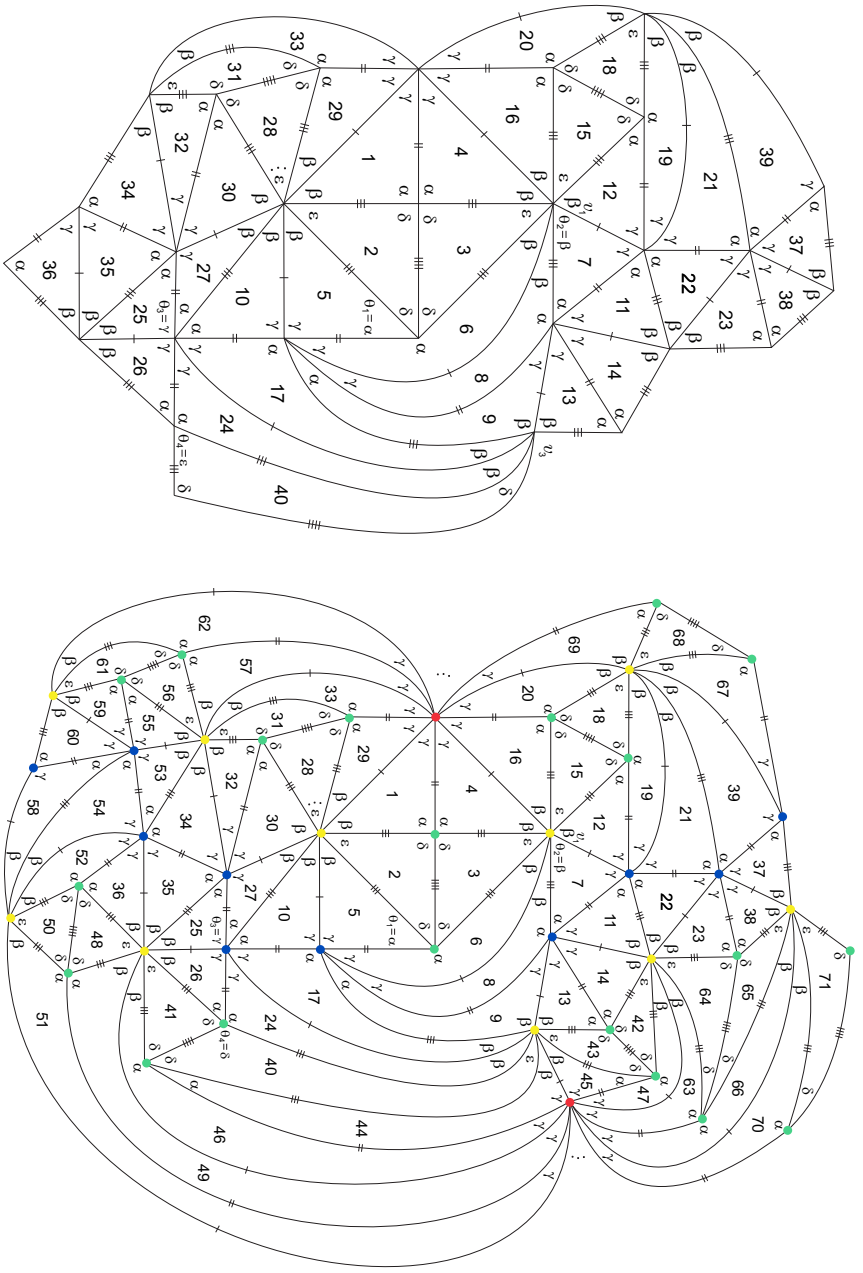

Figure 21: Local configurations.

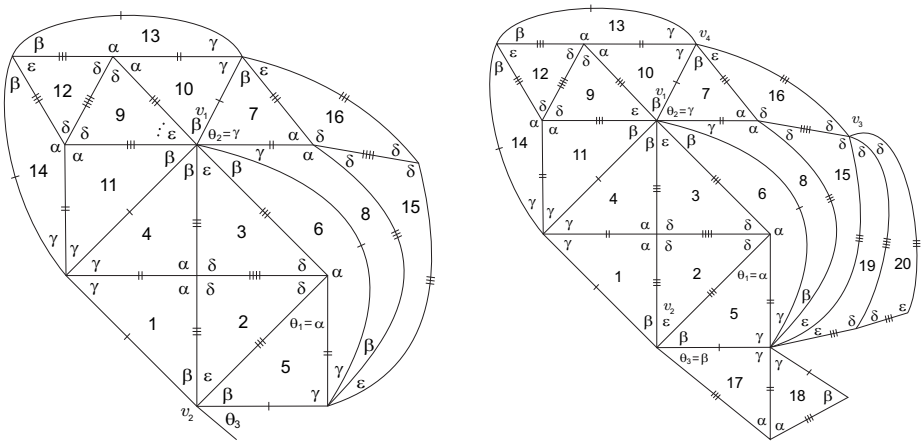

Figure 22: Local configurations.

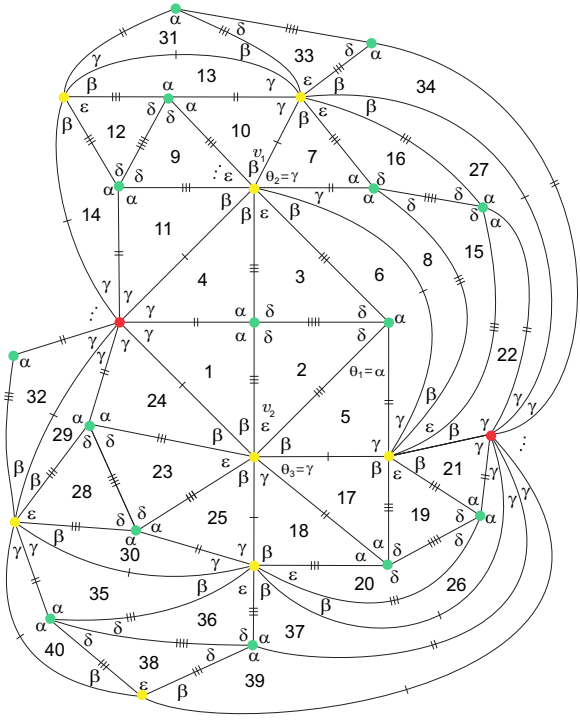

Figure 23: Planar representation of $\mathcal{F}^k_\beta$.

with $\beta \in \left(\beta_{\min}^{1k}, \beta_{\max}^{1k}\right)$, where

$$\beta_{\min}^{1k} = \max\left\{\frac{\pi}{k}, \arccos\left(\frac{1}{2}\sec\frac{\pi}{2k}\right) - \frac{\pi}{2k}\right\} \quad \text{and} \quad \beta_{\max}^{1k} = \frac{(k-1)\pi}{2k}$$

are obtained, respectively, when $\varepsilon = \gamma$ or $\varepsilon = \delta$ and $\alpha = \delta$. Note that if $\varepsilon = \delta$, we get

$$\begin{aligned}
\cos\left(2\beta + \frac{\pi}{k}\right) &= -\cos\frac{\pi}{k}\sec\frac{\pi}{2k}\cos\left(\beta + \frac{\pi}{2k}\right) \\
&\iff \cos\frac{\pi}{2k}\left(2\cos^2\left(\beta + \frac{\pi}{2k}\right) - 1\right) = -\cos\frac{\pi}{k}\cos\left(\beta + \frac{\pi}{2k}\right) \\
&\iff \cos\left(\beta + \frac{\pi}{2k}\right) = \frac{-\cos\frac{\pi}{k} + \sqrt{\cos^2\frac{\pi}{k} + 8\cos^2\frac{\pi}{2k}}}{4\cos\frac{\pi}{2k}} \\
&\iff \cos\left(\beta + \frac{\pi}{2k}\right) = \frac{-\cos\frac{\pi}{k} + \left(2\cos^2\frac{\pi}{2k} + 1\right)}{4\cos\frac{\pi}{2k}} \\
&\iff \cos\left(\beta + \frac{\pi}{2k}\right) = \frac{1}{2}\sec\frac{\pi}{2k}.
\end{aligned}$$

The graph of $\alpha = \alpha_k^1(\beta)$, for $\beta_{\min}^{1k} < \beta < \beta_{\max}^{1k}$, is outlined in Figure 24, for different values of k. Note that the condition $\varepsilon < \delta$ is equivalent to $\alpha < 2\beta + \frac{\pi}{k}$.

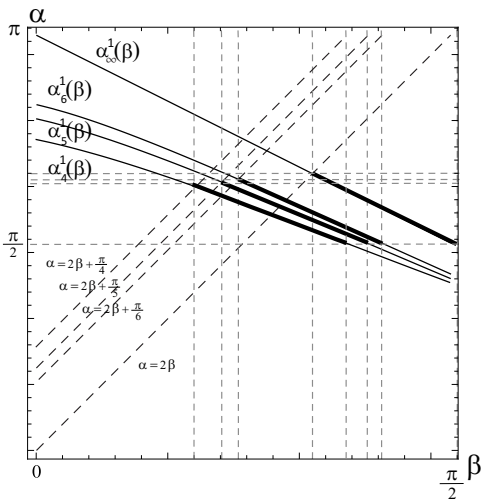

Figure 24: $\alpha = \alpha_k^1(\beta)$, with $\beta_{\min}^{1k} < \beta < \beta_{\max}^{1k}$, and for and for $k = 4, 5, 6, \ldots, \infty$.

3D representations of $\mathcal{F}_\beta^4$, $\mathcal{F}_\beta^5$ and $\mathcal{F}_\beta^6$ are given in Figures 8(k) – 8(m).

Case I.1.2.4.3: If $\theta_2 = \varepsilon$ (Figure 19(a)), at vertex v_1 we must have

(i) $\beta + \beta + k\varepsilon = \pi$, $k \geq 1$,

(ii) $\beta + \beta + \beta + k\varepsilon = \pi$, $k \geq 1$ or

(iii) $\beta + \beta + \gamma + k\varepsilon = \pi$, $k \geq 1$.

Note that in all these cases k must be one, otherwise we reach a vertex with alternate sum $\delta + \delta + \beta = \pi$ and other vertex surrounded in cyclic order by $(\alpha, \varepsilon, \beta, \ldots)$, which is not possible.

In case (i), $\beta + \beta + \varepsilon = \pi$, we obtain the planar representation of Figure 25. We denote

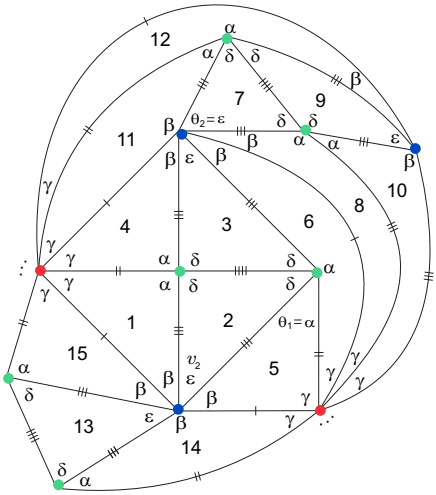

Figure 25: Planar representation of $\mathcal{I}_\beta^k$.

this family of f-tilings by $\mathcal{I}_\beta^k$, where $\alpha + \delta = \pi$, $2\beta + \varepsilon = \pi$ and $k\gamma = \pi$, with $k \geq 3$. Using Equation (3.1), we get

$$\alpha = \alpha_k^2(\beta) = \arccos\left(-\cos\frac{\pi}{k}\cos\beta\right),\ k \geq 3,$$

with

$$\max\left\{\frac{\pi}{k}, \arccos\frac{\sqrt{\cos^2\frac{\pi}{k}+8}-\cos\frac{\pi}{k}}{4}\right\} < \beta < \frac{\pi}{2},$$

where the lower and upper bounds are obtained, respectively, when $\varepsilon = \gamma$ or $\varepsilon = \delta$ and $\alpha = \delta$. The graph of this function is outlined in Figure 26, for different values of k. Note that the condition $\varepsilon < \delta$ is equivalent to $\alpha < 2\beta$.

3D representations of $\mathcal{I}_\beta^k$, for $k = 3, 4, 5$, are illustrated in Figures 9(n) – 9(p).

In case (ii), $\beta + \beta + \beta + \varepsilon = \pi$, using similar arguments applied before, the local configuration extends to the f-tiling $\mathcal{H}$, obtained in Case I.1.2.4.1.

In the last case, by symmetry we obtain the families of f-tilings $\mathcal{F}_\beta^k$ and $\bar{\mathcal{G}}^k$, $k \geq 4$, of Cases I.1.2.4.2 and I.1.2.3(ii), respectively.

Case I.2: With the labeling of Figure 27(a), at vertex v_1 we must have

$$\beta + \delta = \pi \quad \text{or} \quad \beta + \delta < \pi.$$

Case I.2.1: Suppose firstly that $\beta + \delta = \pi$. As $\delta = \beta = \frac{\pi}{2}$ implies $\gamma = \frac{\pi}{2}$, we have $\delta \neq \beta$. If $\delta > \beta$, by Equation (3.1), we conclude that $\alpha > \frac{\pi}{2}$, preventing a feasible assignment for θ_1 and θ_2. In turn, if $\delta < \beta$, we obtain a vertex (v_2) surrounded by four angles δ. As $2\delta < \beta + \delta = \pi$, we would have $2\delta + \rho \leq \pi$, with $\rho \in \{\alpha, \beta, \gamma, \delta, \varepsilon\}$, which is not possible.

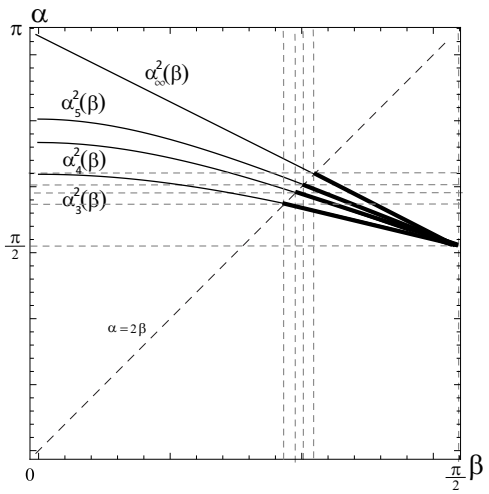

Figure 26: $\alpha = \alpha_k^2(\beta)$, with $\beta_{\min}^{2k} < \beta < \frac{\pi}{2}$, and for $k = 3, 4, 5, \ldots, \infty$.

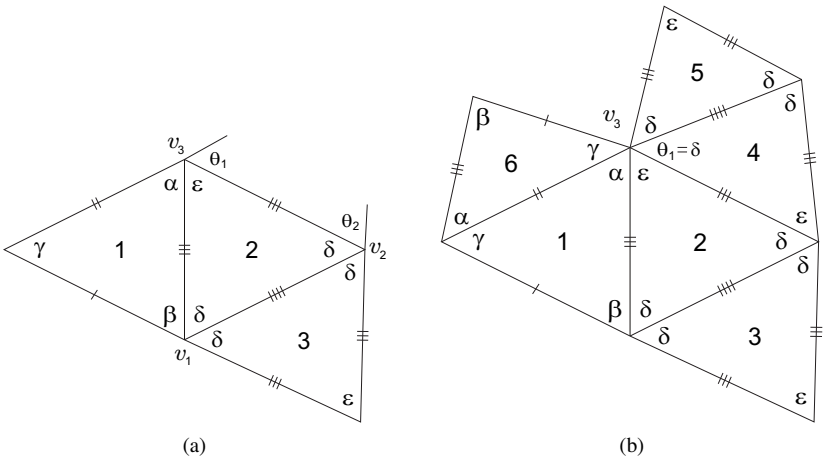

Figure 27: Local configurations.

Case I.2.2: Suppose now that $\beta + \delta < \pi$. As in Case I.2.1, if $\delta \geq \frac{\pi}{2}$, we obtain $\alpha > \frac{\pi}{2}$ and no assignment for θ_1 and θ_2 is possible. Thus, $\delta < \frac{\pi}{2}$ and, as any tiling has necessarily vertices of valency four, we have $\alpha \geq \frac{\pi}{2}$. Now, observing Figure 27(a), we have $\theta_1 \in \{\delta, \varepsilon, \beta\}$.

Case I.2.2.1: If $\theta_1 = \delta$, we obtain the configuration illustrated in Figure 27(b). Vertex v_3 must have valency three, but in this case we get $\alpha + \beta + \delta = \pi = \delta + \varepsilon + \gamma$, implying $\varepsilon > \alpha$, which is not possible.

Case I.2.2.2: If $\theta_1 = \varepsilon$, the last configuration extends uniquely to the one illustrated in Figure 28. Note that at vertex v_4, θ_2 must be β and the vertex must have valency three

($2\beta > \beta+\gamma > \delta$). We denote this family of f-tilings by $\mathcal{J}^k_\beta$, where $\alpha+\varepsilon=\pi$, $2\delta+\beta=\pi$

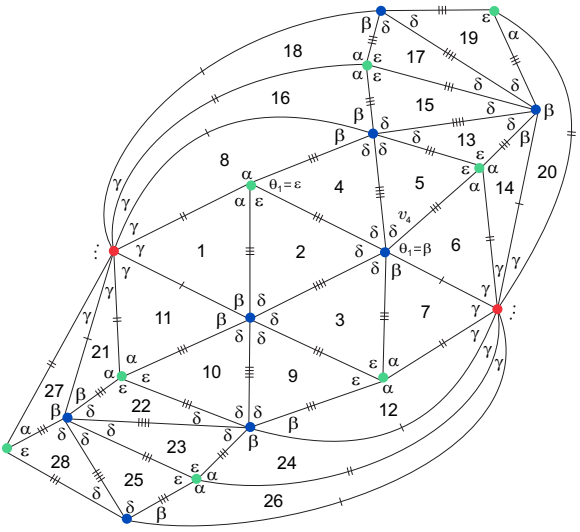

Figure 28: Planar representation of $\mathcal{J}^k_\beta$.

and $k\gamma=\pi$, with $k\geq 4$. Using Equation (3.1) we get

$$\begin{aligned}
&\frac{\cos\frac{\pi}{k}+\cos\alpha\cos\beta}{2\sin\frac{\beta}{2}}=\sin\frac{\beta}{2}(1-\cos\alpha)\\
&\qquad\Longleftrightarrow\ \cos\frac{\pi}{k}+\cos\alpha\left(2\cos^2\frac{\beta}{2}-1\right)=2\left(1-\cos^2\frac{\beta}{2}\right)(1-\cos\alpha)\\
&\qquad\Longleftrightarrow\ \cos\alpha=2\sin^2\frac{\beta}{2}-\cos\frac{\pi}{k}.
\end{aligned}$$

Therefore,

$$\alpha=\alpha^3_k(\beta)=\arccos\left(2\sin^2\frac{\beta}{2}-\cos\frac{\pi}{k}\right),\ k\geq 4,$$

with

$$\frac{\pi}{k}<\beta<2\arcsin\frac{\sqrt{1+8\cos\frac{\pi}{k}}-1}{4},$$

where the lower and upper bounds are obtained, respectively, when $\beta=\gamma$ and $\varepsilon=\delta$. The graph of this function is outlined in Figure 29, for different values of k.

3D representations of $\mathcal{J}^k_\beta$, for $k=4,5,6$, are illustrated in Figures 10(q)–10(s).

Case I.2.2.3: Finally, if $\theta_1=\beta$, at vertex v_3 (see Figure 27(a)) we have $\alpha+\beta\leq\pi$. $\alpha+\beta=\pi=\varepsilon+\gamma$ implies $\varepsilon>\alpha>\frac{\pi}{2}>\delta$, which is a contradiction. As any tiling has necessarily vertices of valency four, we conclude that $\alpha+\beta+k\varepsilon=\pi$, $k\geq 1$, and $\alpha+\delta=\pi$ at vertex v_2, as illustrated in Figure 30, configuration coincident with the one presented in Figure 16(b), which leads to the families of f-tilings $\mathcal{G}^k$ and $\bar{\mathcal{G}}^k$ (Case I.1). □

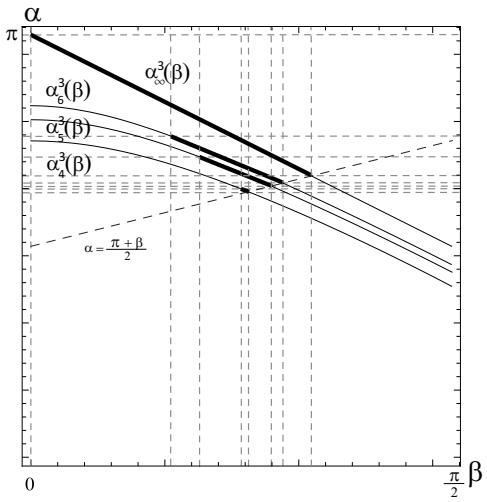

Figure 29: $\alpha = \alpha_k^3(\beta)$, with $\frac{\pi}{k} < \beta < \beta_{\max}^{3k}$, and for $k = 4, 5, 6, \ldots, \infty$.

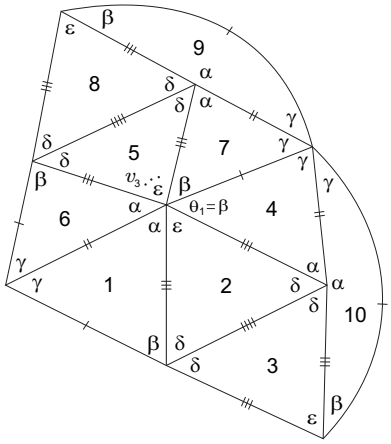

Figure 30: Local configuration.

References

[1] A. M. R. Azevédo Breda, A class of tilings of S^2, *Geom. Dedicata* **44** (1992), 241–253, doi: 10.1007/bf00181393.

[2] A. Breda, R. Dawson and P. Ribeiro, Spherical f-tilings by two noncongruent classes of isosceles triangles – II, *Acta Math. Sin. (English Series)* **30** (2014), 1435–1464, doi:10.1007/s10114-014-3302-5.

[3] R. J. M. Dawson, Tilings of the sphere with isosceles triangles, *Discrete Comput. Geom.* **30** (2003), 467–487, doi:10.1007/s00454-003-2846-4.

[4] R. J. M. Dawson and B. Doyle, Tilings of the sphere with right triangles I: The asymptotically right families, *Electron. J. Combin.* **13** (2006), #R48, `http://www.combinatorics.org/ojs/index.php/eljc/article/view/v13i1r48`.

[5] R. J. M. Dawson and B. Doyle, Tilings of the sphere with right triangles II: The $(1, 3, 2)$, $(0, 2, n)$ subfamily, *Electron. J. Combin.* **13** (2006), #R49, http://www.combinatorics.org/ojs/index.php/eljc/article/view/v13i1r49.

[6] A. M. d'Azevedo Breda and A. F. Santos, Dihedral f-tilings of the sphere by spherical triangles and equiangular well-centered quadrangles, *Beiträge Algebra Geom.* **45** (2004), 447–461, https://www.emis.de/journals/BAG/vol.45/no.2/8.html.

[7] A. M. R. d'Azevedo Breda and P. dos Santos Ribeiro, Spherical f-tilings by two non congruent classes of isosceles triangles – I, *Math. Commun.* **17** (2012), 127–149, https://hrcak.srce.hr/82991.

[8] S. A. Robertson, Isometric folding of Riemannian manifolds, *Proc. Roy. Soc. Edinburgh Sect. A* **79** (1978), 275–284, doi:10.1017/s0308210500019788.

[9] Y. Ueno and Y. Agaoka, Classification of tilings of the 2-dimensional sphere by congruent triangles, *Hiroshima Math. J.* **32** (2002), 463–540, http://projecteuclid.org/euclid.hmj/1151007492.